CORRELATIONS BETWEEN FOAMING INDEX AND SLAG PROPERTIES IN SMELTING REDUCTION OF IRON OXIDE

A.K. Jouhari, R.K. Galgali, R.C. Gupta* and H.S. Ray

Regional Research Laboratory
Bhubaneswar - 751 013
*Department of Metallurgical Engineering
Institute of Technology, Banaras Hindu University
Varanasi - 221 005

Abstract

In the present work, data of eighteen experiments have been discussed to develop a correlation between foaming index and slag properties. The experiments have been carried out under different conditions in a plasma reactor of 50 kW capacity. Reduction of FeO containing slags has been carried out in a graphite crucible and the reduction takes place by carbon drawn from the crucible surface only. No additional external reductant has been used. The data have been analyzed for initial stages of reduction to estimate gas velocity in the reactor and the foaming index is calculated from foam height and estimation of the volume of CO gas generated due to FeO reduction. It is shown that variations in foaming index (Σ, sec) and rate constant (k, min^{-1}) are related to variations in initial FeO percentage of slag, slag height and CaF_2 content.

INTRODUCTION

Smelting reduction technology involves substantial reduction of iron oxide rich slag in the liquid state either by solid carbon or carbon saturated liquid iron bath. This reaction also takes place in the hearth of the blast furnace, in oxygen blown converter and arc furnaces when sponge iron is used. The smelting reduction process, which is based upon use of non-coking coals primarily, is a process of judicious combination of pre-reduction of iron ore, FeO reduction and post combustion of CO generated in the process.

Early investigations on reduction of FeO in molten slag reported by Philbrook and co-workers [1,2] and Yusheng and Ting [3] presented some critical reviews and useful data. Various workers generally believe that amongst the kinetic steps, including formation of metallic iron and gas bubbles, only the following are likely to be slow and rate controlling.

(a) Slag-gas reaction involving, (i) transfer of FeO in slag, and (ii) chemical reaction at slag-gas interface, and

(b) Carbon-gas reaction involving chemical reaction at carbon-gas or metal-gas interface.

The process is complex and at least three phases would be present. Extensive emulsion or foam formation and consequent dispersion of phases make reaction geometry complicated and interfacial areas uncertain [4].

Sato et al. [5] have given a comprehensive review on reduction of FeO in slag by solid carbon as well as by carbon in molten iron. Reduction rates were calculated from the amount of CO gas evolved. They have reported reduction rates by solid carbon as 2.1-8.2 x 10^{-5} mole.FeO/cm^2-sec at 1420-1620°C.

Recently, Utigard and Zamalloa [6] have published a comprehensive review on some aspects of foaming. Systematic studies on foaming slags were initiated by Cooper and Kitchener [7] some forty years ago. They worked on the CaO-SiO$_2$ system, with small additions of P$_2$O$_5$ in the temperature range 1475-1725°C using molybdenum crucible and measured the time required for foam to decay from an arbitrary height after the foam reached a steady state. No stable foam was observed but the foam height increased with additions of P$_2$O$_5$. The foam life increased with decreasing temperature

and slag basicity. Subsequently, Swisher and McCabe [8] studied the influence of Cr_2O_3 on foaming of $CaO-SiO_2$ slags and observed that Cr_2O_3 enhanced foam life.

Further studies were reported by Zhang and Fruehan [9] who investigated slag foaming using bubbles smaller than those used in the previous studies. These bubbles were generated by argon gas injection with the nozzle of multiple small orifices and by the slag-metal interfacial reaction of FeO in the slag with carbon in liquid iron. The foam stability for a bath smelting type of slag ($CaO-SiO_2-Al_2O_3-FeO$) was determined for different bubble sizes. The average diameter in the foam was measured by a X-ray video technique. When the foam was generated by the slag-metal interfacial reaction at 1450^oC, it was found that the average bubble diameter varied from less than 1 to more than 5 mm depending on the function of the sulphur activity in the carbon saturated liquid iron. The foaming index was found to be inversely proportional to the average bubble diameter. These workers have also worked on use of carbonaceous particles such as coke/coal char for controlling slag foaming [10]. It was concluded that the anti-foam effect of coke/coal char particles was primarily due to the non-wetting nature of the carbonaceous materials with respect to the liquid slag.

Laboratory investigations reported in the literature have employed slag composition in three distinct regions, namely, 0-20 %, 20-80 % and 80-100 % FeO. The present work examines the behaviour of the middle category which is the most important from industrial point of view. The following process variables affect the reduction rate : initial FeO concentration, temperature, crucible-slag interfacial area, slag basicity, initial slag height, addition of CaF_2, etc. These parameters also influence the foaming behaviour. Therefore, it is necessary to study the influence of these process variables on reduction and foaming. It is also necessary to understand the role of slag properties during reduction and foaming so as to collect useful information for design and operation of a reactor.

In the present work experiments have been conducted to study reduction of slags containing 20-60 % FeO in the CaO/SiO_2 ratio of 0.86-1.43 at temperature ranging from 1450-1650 ^OC , in a graphite crucible of varying diameter (7-11 cm), in an indigenously

built plasma reactor of 50 kW capacity. The initial slag height has been varied in the range 2.4 to 4.2 cm and calcium fluoride addition has been varied between 0-2 %.

EXPERIMENTAL

The plasma reactor used is of pot type with a graphite crucible serving as the reactor chamber. It is similar to the one reported earlier [11]. Figure 1 shows a schematic diagram of the reactor. The side walls are zircon coated and the crucible is provided with a tap hole and a graphite spout for discharging both metal and slag. While the crucible itself forms one electrode (anode), a movable vertical graphite rod functions as the cathode. The top electrode, actuated by a rack and pinion mechanism, has an axial hole for passing the plasma forming gas. The ends of both the electrodes are water cooled. The entire assembly has been designed for 50 kW dc power supply but normally 12.50 to 14 kW is used in the present work, the temperature being controlled by the power input to within $\pm 50^{o}C$ approximately.

Initially, the crucible was preheated for a period of 10 minutes under argon plasma generated by passing 2 l/min argon through the axial hole of the cathode. Lime-silica slag was placed in the crucible after shorting the electrodes. The power to the reactor was switched on, cathode was moved away and a stable argon plasma was established. The slag was melted and homogenized within 10 minutes. Power was switched off, the liquid slag stirred and slag height measured by dipping a steel rod. Length of the slag layer sticking to the rod was taken as slag height. The required quantity of iron ore was then added to the molten slag and time was noted as zero time. At an interval of four minutes, power to the reactor was switched off again, the height of foamed slag was measured and slag samples were taken for FeO analysis. The foam height was calculated by deducting the initial slag height from the height of foamed slag.

The total experimental time was 60 minutes including 10 minutes for preheating of the crucible and 10 minutes for melting of slag. At the end of the experiment, the metal and the slag were tapped. The temperature of the bath was measured with the help of an Infrared Pyrometer. During tapping, the plasma was kept on.

RESULTS AND DISCUSSION

The maximum initial FeO level in the slag is established only after the reduction of Fe_2O_3 to FeO and dissolution of FeO in slag. Accordingly, a plot of FeO content versus time goes through a peak. The foam height, however, continues to build well beyond this peak. Figure 2 shows data of two experiments to illustrate this. It may be noted that while the maximum FeO level, and consequently, the maximum reaction rate establishes after about 4-8 minutes, the maximum foam height requires 16-24 minutes. As expected, the dissolution time is more at lower temperatures.

Bikerman [14] introduced the concept of foaming index to quantify slag foaminess. He defined the term foaming index (Σ) based on the assumption that the foam formed at steady state was proportional to the gas flow rate. The constant of proportionality was named as foaming index. If the cross section area of a reactor is constant, Σ can be expressed in terms of the foam height(h) in cm and the superficial gas velocity (v) in cm/sec. It gives the residence time or travelling time of gas in the slag.

$$\Sigma = h/v \qquad\qquad (1)$$

Estimation of Slag Properties

For analyzing the experimental data in terms of dimensionless numbers we need to know the properties of slag. Methods of estimating density, viscosity and surface tension values on the basis of slag composition and temperature are outlined here. The relevant equations used are follows :

Density

From the data available in the literature [15], one can obtain the following correlations to estimate density ρ, in kg/m^3.

$$\rho = 2693 + 13 \ (pct \ FeO) \qquad\qquad (2)$$

This is valid when CaO/SiO_2 equals 1.25-1.30.

Additionally, $\rho = 2970 + 145 \, (CaO/SiO_2)$ (3)

for 35 pct FeO in slag.

Viscosity

Viscosity of slag has been estimated using Urbain's model [16] which is based on experimental data for pure binary and ternary melts.

The viscosity of slag, μ (poise) has been given by the following equations.

$\mu = AT \exp (1000 \, B/T)$ (4)

where, A and B are constants defined by another equation and T is temperature, Kelvin.

$-\ln A = mB + n$ (5)

where, $m = 0.29$ and $n = 11.57$

B is estimated from the composition of the slag using the following procedure.

All cations are empirically classified into three classes such as glass former, modifier and amphoteric.

Glass former	:	Cation Si^{4+}
Modifier	:	Cations, Mg^{++}, Ca^{++}, Fe^{++}
Amphoteric	:	Cations, Al^{3+}, Fe^{3+} which may act either as glass former or modifier

The chemical analysis of slag gives weight. percent of each component which is then converted to mole and then to mole fraction (N). Two convenient composition parameters are defined as follows.

$X = N \, (SiO_2)$ (6)

$\alpha' = MO \, / \, [MO + N \, (Al_2O_3)]$ (7)

where, MO   = Σ (mole fraction of modifier oxides)

          = $N \, (CaO) + N \, (MgO) + N \, (FeO)$

The constant B is represented by the following polynomial equation.

$B = B_o + B_1 X + B_2 X^2 + B_3 X^3$ (8)

$$B_i = a(i) + b(i).\alpha' + c(i).\alpha'^2 \tag{9}$$

with $i = 0, 1, 2, 3$

It is possible to calculate B for two ternaries, such as B (Mg) for ternary SiO_2-Al_2O_3-MgO and B (Ca) for ternary CaO-SiO_2-Al_2O_3 and obtain mean of B by considering B (Mg) and B (Ca) using the mole fractions N (MgO) and N (CaO).

The parameters a, b and c are given in Table I.

When CaF_2 is added to the slag, its dissociation scheme gives the equivalent of 3 MO. Calcium fluoride is considered as modifier cation.

Surface tension

The surface tension, γ, has been estimated taking into account molar composition of slag, pct CaO, SiO_2 and FeO.

$$\gamma = N_1\gamma_1 + N_2\gamma_2 + N_3\gamma_3 \tag{10}$$

where, N_1, N_2, N_3 are molar fractions and γ_1, γ_2, γ_3 are surface tension values for each component. These properties are taken at $1570^{\circ}C$ [17] and then temperature correction has been made.

The three components CaO, SiO_2, FeO put together constitute more than 90 pct by weight. The other elements like Al_2O_3 and MgO have been neglected in estimation of the surface tension.

Table II gives the slag properties estimated using slag composition at bath temperature measured during different experiments.

To study the relationship between foaming index with slag properties, Jiang and Fruehan [15] have defined two dimensionless numbers π_1 and π_2 as follows.

$$\pi_1 = \Sigma \, g\mu/\gamma \tag{11}$$

$$\pi_2 = \rho\gamma^3/g\mu^4 \tag{12}$$

Here Σ, g, μ, ρ, γ are foaming index, acceleration due to gravity, viscosity, density and surface tension respectively. It may be noted that π_1 contains the term Σ which is experimentally determined whereas all other parameters, i.e. slag properties are estimated from the available literature. The dimensionless term, π_2 is inverse of Morton number

which describes the balance between gravitational, viscous and surface tension forces. It is generally used to describe the velocity of bubbles in liquids.

Figure 3 gives the plot of $\log \pi_2$ versus $\log \pi_1$ for all the experiments. The slope and intercept are found to be -1.98 and 6.34 respectively, using the least square method. In view of the various uncertainties in estimating the values of slag properties, the slope can be taken as -2.0. Thus the relationship is written as follows.

$$\log \pi_2 = -2 \log \pi_1 + 6.34 \tag{13}$$

From this the following correlation is derived.

$$\Sigma = 470 \, \mu/(\rho\gamma)^{0.5} \tag{14}$$

It is interesting to compare this correlation with that given by Jiang and Fruehan [15] in the literature which is written as follows.

$$\Sigma = 115 \, \mu/(\rho\gamma)^{0.5} \tag{15}$$

In an earlier work, Ito and Fruehan [12,13] had reported a higher value of the constant (570) which they subsequently revised to 115 saying that the larger value presumably arose out of incorrect estimation of slag properties. Therefore, in this case also, the value of the constant does not have any absolute significance and it is result of using some particular correlations. There are several uncertainties in the process of estimation and these have been discussed elsewhere [18].

From the FeO reduction curve, one obtains the α-t plots where α is fraction of FeO in slag reacted. Zero time was taken after dissolution of FeO in slag was complete and the reduction of FeO began. From α-t data the rate constant k in min^{-1} was estimated by making $-\ln(1-\alpha)$ vs t plots for first order kinetics. It was found that the FeO reduction reaction in molten slag followed this first order kinetics. The detailed analysis is given elsewhere [18].

Figure 4 to Fig. 6 show the plots of rate constant and foaming index for increase of FeO in slag, increase in initial slag height and addition of CaF_2 in slag respectively. From these plots, the following observations may be made.

a)   Increase of FeO in slag results in higher rate constant values and lower values of foaming index.

b)   Increase in initial slag height increases rate constant and also the foaming index.

c)   Addition of CaF_2 in slag also increases rate constant but it lowers the foaming index

It may be observed that all the three plots show linear relationship. These plots will help in assessing reaction rates and foaming behaviour provided other parameters are known.

CONCLUSIONS

The main conclusions of the present study are as follows.

1.   The experimental data give rise to the following correlation between the dimensionless numbers, $\pi_1 = \Sigma g \mu / \gamma$ and $\pi_2 = \rho \gamma^3 / g \mu^4$.

$$\log \pi_2 = -2 \log \pi_1 + 6.34$$

From this correlation one can also derive the following relationship.

$$\Sigma = 470 \, \mu / (\rho \gamma)^{0.5}$$

The equation indicates that the foaming index is directly proportional to the viscosity and inversely proportional to the square root of the product of density and surface tension.

2.   The preceding conclusions indicate that foaming behaviour is related to the slag properties which can be estimated on the basis of slag composition and temperature. The correlations may provide useful guidance for design and operation of reactors for smelt reduction.

3.   The effect of some variables is as follows.

(a) As FeO content in slag increases, the rate constant, k increases and foaming index, Σ decreases.

(b) As initial slag height increases, both rate constant, k and the foaming index, Σ increases.

(c) Addition of CaF_2 results in increase in rate constant, k and decrease in foaming index, Σ.

ACKNOWLEDGEMENTS

NOMENCLATURE

|		
d	=	crucible diameter, cm
g	=	acceleration due to gravity, m/sec^2
h	=	foam height, cm
k	=	rate constant, min^{-1}
N	=	mole fraction
T	=	temperature, K
v	=	superficial gas velocity, cm/sec
X	=	a fraction
α'	=	fraction of modifier oxides
ρ	=	density of slag, kg/m^3
μ	=	viscosity of slag, $N\text{-}s/m^2$
γ	=	surface tension of slag, N/m
Σ	=	foaming index, sec = h/v
π_1	=	dimensionless number = $\Sigma\, g\mu/\gamma$
π_2	=	dimensionless number = $\rho\gamma^3/g\mu^4$

REFERENCES

1.   W.O. Philbrook and L.D. Kirkbride, *Trans. AIME*, 1956, vol.206, p.351.

2.   S.K. Tarbi and W.O. Philbrook, *Trans. Met. Soc. AIME*, 1967, vol.239, p.1005.

3.   Z. Yusheng and D. Ting, Proc. Shenyang International Symp. on Smelting Reduction, Chinese Society of Metals, Sept.3-5, 1986, pp.147-159.

4.   A. Ghosh, in "Production of Liquid Iron Using Coal", (Eds. H.S. Ray, D.N. Dey, R.K. Paramguru and A.K. Jouhari), Allied Publishers, New Delhi, 1994, pp.139-142.

5.   A. Sato, G. Aragane, K. Kamihira and S. Yashimatsu, *Trans. ISIJ*, 1987, vol.27, pp.789-796.

6.   T.A. Utigard and M. Zamalloa, *Scand. J. of Metallurgy*, 1993, vol.22, pp.83-90.

7.   C.F. Cooper and J.A. Kitchener, *JISI*, 1959, vol.193, pp.48-55.

8.   J.H. Swisher and C.L. McCabe, *Trans. TMS-AIME*, 1964, vol.230, pp.1669-1675.

9.   Y. Zhang and R.J. Fruehan, *Metallurgical and Material Transactions B*, 1995, vol.26B, pp.803-812.

10.   Y. Zhang and R.J. Fruehan, ibid, pp.813-819.

11.   R.K. Galgali, U. Syamaprasad, S.K. Mishra and B.C. Mohanty, *Trans. IIM*, 1988, vol.41, pp.489-491.

12.   K. Ito and R.J. Fruehan, *Met. Trans.*, 1989, vol.20B, pp.509-514.

13.   K. Ito and R.J. Fruehan, ibid, pp.515-520.

14.   J.J. Bikerman, Foams, *Springer Verlag*, Berlin, 1973, pp.65-97 and 149-158.

15.   R. Jiang and R.J. Fruehan, *Met. Trans.*, 1991, vol.22B, pp.481-489.

16.   G. Urbain, *Steel Research*, 1987, vol.58(3), pp.111-116.

17.	The Making Shaping and Treating of Steel, United States Steel, Tenth Edition, 1985, p.438 and 423.

18.	A.K. Jouhari, Foaming Behaviour of FeO Containing Slags During Reduction by Solid Carbon, Ph.D.Thesis, Banaras Hindu University, 1997.

FIGURE CAPTIONS

Fig.1.	Schematic diagram of plasma reactor.

Fig.2	Plots showing simultaneous variation of FeO concentration in slag and slag height with reaction time.

Fig.3	Plot of log π_2 vs log π_1

Fig.4	Plots of foaming index and rate constant for variation of FeO in slag

Fig.5	Plots of foaming index and rate constant for variation in initial slag height.

Fig.6	Plots of foaming index and rate constant for addition of CaF_2 in slag.
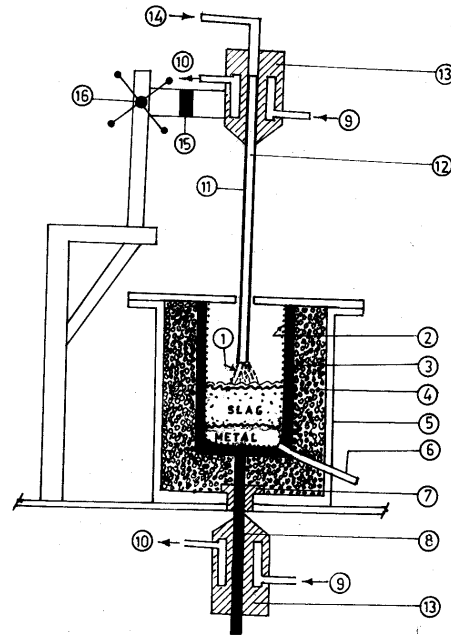
1. Plasma 2. Zircon Coating 3. Graphite Crucible 4. Bubble Alumina
5. M. S. Casing 6. Tap hole 7. Alumina Bush 8. Bottom Graphite Electrode
9. Water Inlet 10. Water Outlet 11. Top Graphite Electrode 12. Axial Hole
13. Copper Block 14. Plasma Forming Gas 15. Electrical Insulation
16. Rack & Pinion Mechanism.

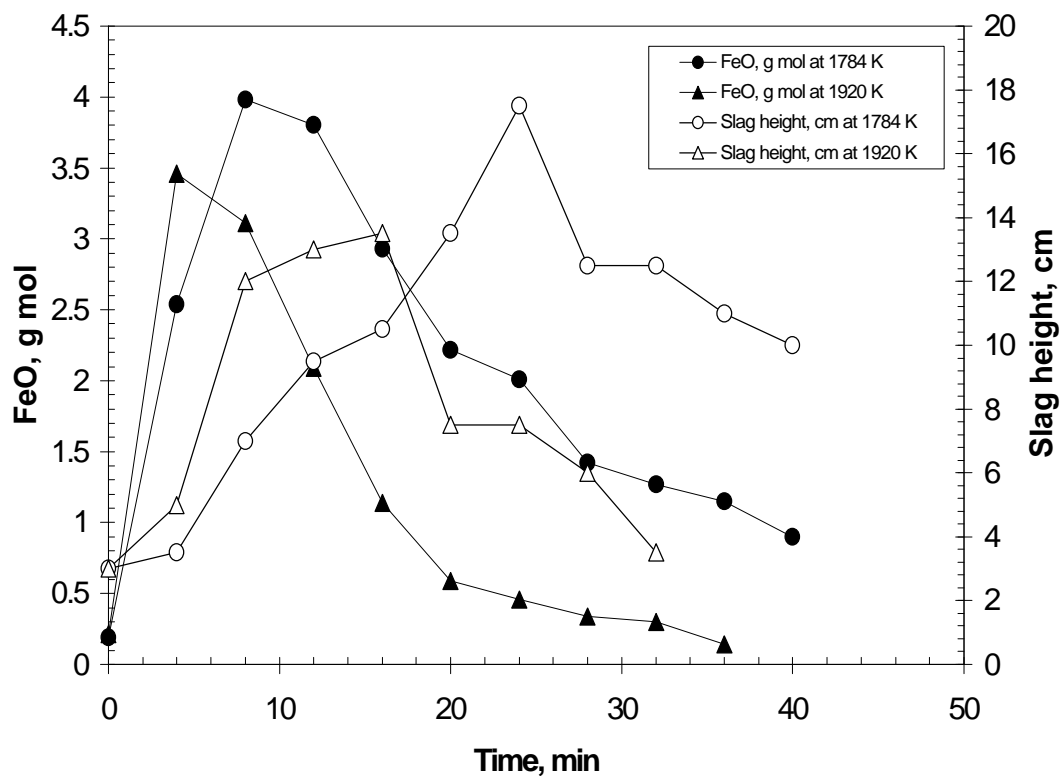Fig. 1 Schematic diagram of a plasma reactor.

Fig.2 : Plots showing simultaneous variation of FeO concentration
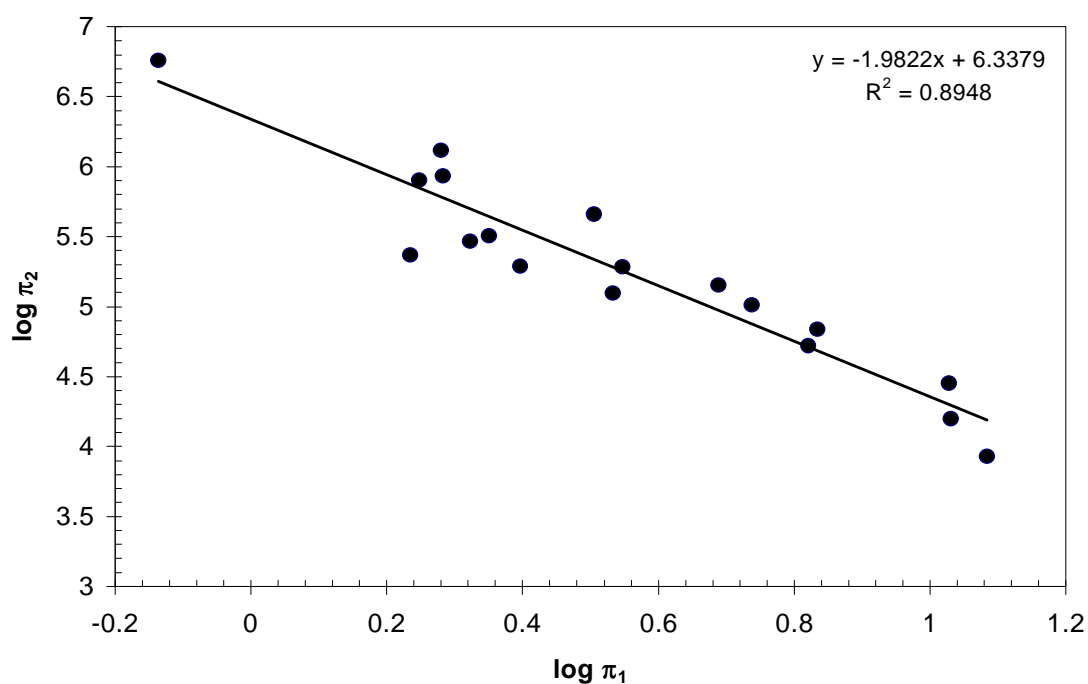in slag and slag height with reaction time

Fig.3 : Plot of log π_2 vs log π_1

$y = -1.9822x + 6.3379$
$R^2 = 0.8948$

CaO/SiO$_2$ = 1.29

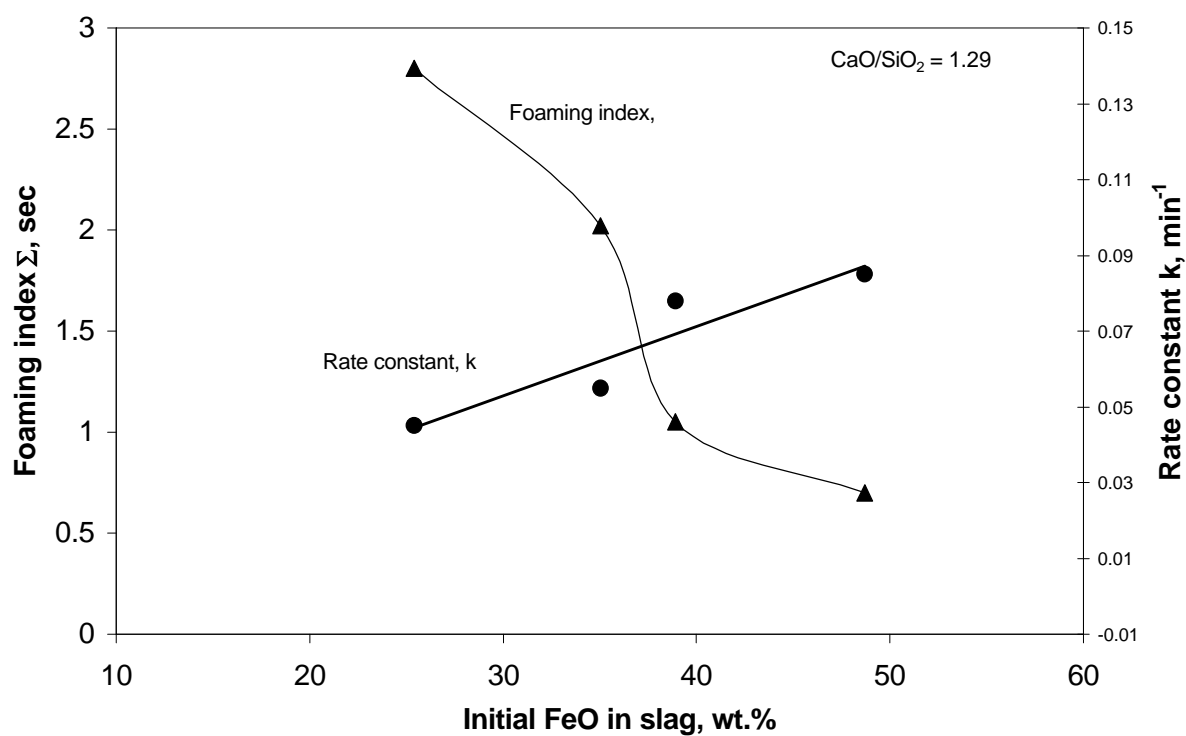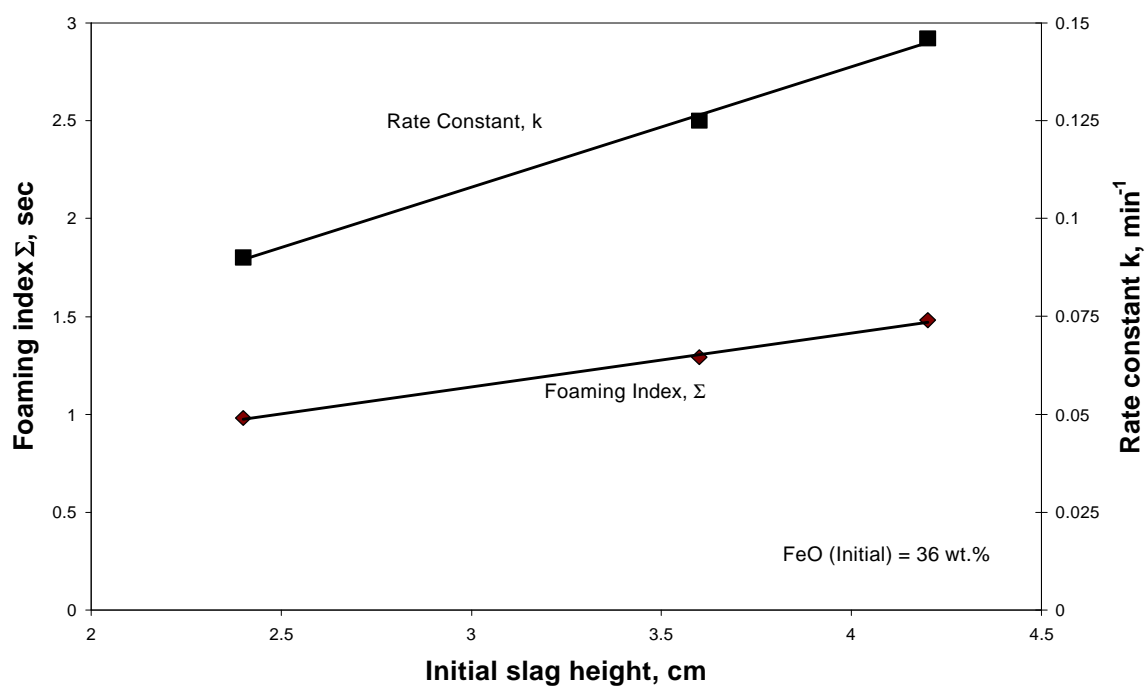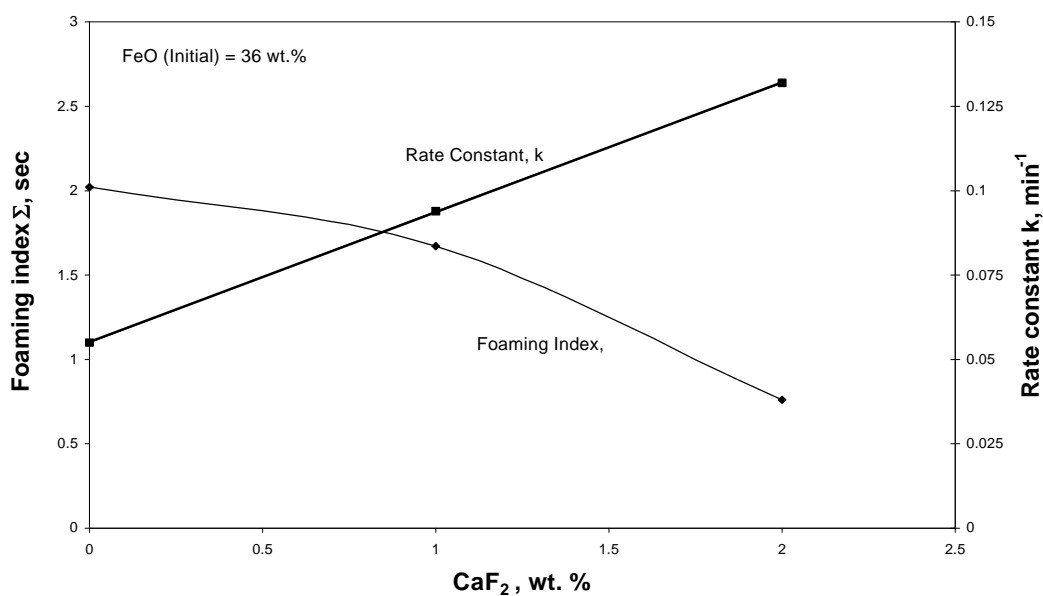Foaming index,

Rate constant, k

Fig.4 : Plots of foaming index and rate constant for variation of FeO in slag

Fig.5 : Plot of foaming index and rate constant for variation in initial slag height

Fig.6 : Plots of foaming index and rate constant for addition of CaF_2 in slag

Table I : Parameters a, b and c

	a(i)	b(i)		c(i)	
i	Mg, Ca	Mg	Ca	Mg	Ca
0	13.2	15.9	41.5	-18.6	-45
1	30.5	-54.1	-117.2	33	130
2	-40.4	138	232.1	-112	-298.6
3	60.8	-99.8	-156.4	97.6	213.6

Table II : Density, viscosity and surface tension of the slag

Sl. No.	Initial FeO, pct	CaO/SiO$_2$ (Actual)	Bath temp., Kelvin	Density, kg/m^3	Viscosity, N-sec/m^2	Surface tension, N/m
1	17.99	1.29	1723	2930	0.249	0.479
2	25.41	1.29	1755	3030	0.187	0.482
3	35.03	1.29	1753	3150	0.165	0.494
4	38.91	1.29	1809	3210	0.119	0.492
5	48.69	1.29	1996	3340	0.050	0.472
6	38.28	1.43	1882	3180	0.082	0.482
7	36.20	1.26	1784	3150	0.138	0.487
8	40.45	0.96	1871	3110	0.099	0.460
9	37.10	0.86	1997	3090	0.066	0.428
10	29.16	1.33	1780	3150	0.152	0.485
11	33.11	1.27	1806	3150	0.126	0.481
12	34.94	1.24	1681	3150	0.225	0.502
13	33.05	1.25	1920	3150	0.078	0.462
14	35.01	1.30	1829	3150	0.117	0.482
15	37.80	1.26	1787	3150	0.132	0.490
16	35.73	1.29	1843	3150	0.105	0.480
17	37.08	1.30	1821	3150	0.094	0.481
18	36.90	1.29	1754	3150	0.112	0.486